Solar and atmospheric neutrino oscillations with three flavors

Mohan Narayan, M. V. N. Murthy, G. Rajasekaran, and S. Uma Sankar*
Institute of Mathematical Sciences, Madras 600 113, India
(Received 8 May 1995)

We analyze the solar and the atmospheric neutrino problems in the context of three flavor neutrino oscillations. We assume a mass hierarchy in the vacuum mass eigenvalues $\mu_3^2 \gg \mu_2^2 \geq \mu_1^2$, but make no approximation regarding the magnitudes of the mixing angles. We find that there are small but continuous bands in the parameter space where the constraints imposed by the current measurements of ^{71}Ga, ^{37}Cl, and Kamiokande experiments are satisfied at the 1σ level. The allowed parameter space increases dramatically if the error bars are enlarged to 1.6σ. The electron neutrino survival probability has a different energy dependence in different regions of the parameter space. Measurement of the recoil electron energy spectrum in detectors that use ν-e scattering may distinguish between some of the allowed regions of parameter space. Finally we use the results for the parameter space admitted by the solar neutrinos as an input for the atmospheric neutrino problem and show that there exists a substantial region of parameter space in which both problems can be solved.

PACS number(s): 14.60.Pq, 95.30.Cq, 96.40.Tv, 96.60.Jw

I. INTRODUCTION

The solar neutrino problem has been an interesting and intriguing phenomenon in neutrino physics for a long time. The different solar neutrino experiments observe differing fractions of the neutrino flux predicted by the standard solar model (SSM) [1,2]. The oldest of the solar neutrino experiments is the ^{37}Cl experiment at Homestake. Its energy threshold is 0.814 MeV and it can detect the neutrinos from ^{7}Be ($E_\nu = 0.862$ MeV) and ^{8}B ($E_\nu \leq 14.02$ MeV) reactions. In the standard solar model (SSM) of Bahcall and Pinsonneault [3], the capture rate in the ^{37}Cl experiment is predicted to be 8.0 ± 1.0 solar neutrino units (SNU). However, the measured rate is only [4]

$$R_{\mathrm{Cl}} = 2.55 \pm 0.25 \text{ SNU}. \tag{1}$$

The water Cherenkov detector at Kamioka, with a threshold of 7.5 MeV, can detect only the neutrinos from the upper end of the ^{8}B spectrum and the Kamioka result [5] is

$$y_{\mathrm{Kam}} = \frac{R_{\mathrm{Kam}}}{R_{\mathrm{Kam\ SSM}}} = 0.51 \pm 0.07, \tag{2}$$

which is the ratio of the observed neutrino flux to that predicted by the SSM. The gallium experiments SAGE and GALLEX, with energy threshold of 0.233 MeV, can detect the neutrinos coming from the dominant p-p reaction ($E_\nu \leq 0.42$ MeV) as well as the neutrinos from ^{7}Be and ^{8}B reactions. Their measured rates are [6,7]

$$R_{\mathrm{SAGE}} = 69 \pm 11 \pm 6 \text{ SNU},$$

$$R_{\mathrm{GALLEX}} = 79 \pm 10 \pm 6 \text{ SNU},$$

and the average is

$$R_{\mathrm{Ga\ avg}} = 74 \pm 8 \text{ SNU} \tag{3}$$

as opposed to the SSM prediction of 131.5 SNU.

A rough model independent analysis of these results indicates that the low energy neutrinos from the p-p reaction suffer very little suppression whereas the higher energy neutrinos are suppressed to a large extent [1,8]. Recently it was pointed out that, if neutrinos have no properties beyond those in the standard electroweak model (i.e., if they are massless), the measurement of Kamiokande, together with that of the ^{37}Cl experiment, implies that the ^{7}Be neutrinos must be suppressed by more than 90% [9,10].

In addition there exists an anomaly in the ratio of observed muon neutrinos to electron neutrinos in the earth's atmosphere. These neutrinos are produced from the decay of $\pi^\pm$ and $K^\pm$ which are in turn produced by cosmic rays interacting with the atmosphere. The ratio is roughly 2 as suggested by the Monte Carlo calculations whereas both Kamioka [11] and IMB [12] report that the ratio is only about half of that predicted by the Monte Carlo calculations. The results for this ratio are also available from three other groups using tracking detectors, namely, the NUSEX [13], Frejus [14], and SOUDAN-II [15] Collaborations. The data from the NUSEX Collaboration seem to be in agreement with the no-anomaly situation. A similar conclusion is obtained from the Frejus data if all the contained events are considered. However, if only fully contained results are taken into consideration, there is a suppression. The SOUDAN-II results are consistent with the results obtained with water Cherenkov detectors. It should be noted that the

*Present address: Department of Physics, Indian Institute of Technology, Powai, Bombay 400 076, India.

statistics in the tracking experiments is not as high as in the water Cherenkov experiments. Evidently any solution of the solar neutrino puzzle must incorporate simultaneously a solution of the atmospheric neutrino problem [16].

A satisfactory solution to the solar neutrino problem should be able to explain not only the total deficit that is observed but the differential suppression observed at low and high energies. Solutions based on astrophysics or nuclear physics ascribe the deficit to smaller solar core temperature or smaller cross sections for the nuclear reactions taking place in the sun. Recent model-independent analyses suggest that these solutions cannot describe the results of ^{37}Cl and Kamiokande simultaneously [2,8]. Particle physics based solutions attempt to account for the deficit by assuming that the neutrinos have interactions beyond those of the standard electroweak model. If the neutrinos possess small mass, an electron neutrino can oscillate into a neutrino of another flavor [17]. The amplitude of oscillation is a function of the mass squared differences, the mixing angles between neutrino flavors, and the neutrino energy. If one of the mass square differences is of the order of the effective mass squared arising from ν_e-e interaction, the matter effects can enhance the mixing to its maximal value, and the amplitude for ν_e oscillating into another flavor will be very large [18]. This is the so called Mikheyev-Smirnov-Wolfenstein (MSW) effect.

Matter-enhanced oscillations have been studied thoroughly in the scenario where only two flavors, ν_e and ν_μ, mix with each other [19–21]. The vacuum oscillation here is controlled by two parameters, the mass square difference $\delta_{21} = m_2^2 - m_1^2$ and the mixing angle ω. The matter effect is taken into account by adding to the mass squared of ν_e the term

$$A(r) = \sqrt{2}\, G_F\, n_e(r) 2E, \tag{4}$$

which is proportional to the electron number density in the Sun, $n_e(r)$, where r is the radial distance from the center of the Sun. The maximum value of A occurs at the core and is roughly $10^{-5}E$ eV^2, where E is the neutrino energy in MeV. The mixing angle ω_m in the presence of matter is given by

$$\cos 2\omega_m = \frac{\delta_{21}\cos 2\omega - A}{\sqrt{(\delta_{21}\cos 2\omega - A)^2 + (\delta_{21}\sin 2\omega)^2}}. \tag{5}$$

The MSW resonance condition is

$$A = \delta_{21}\cos 2\omega. \tag{6}$$

Note that, if the resonance condition is to be satisfied, $A_{\rm core} > \delta_{21}\cos 2\omega$, which implies that $\omega_m > \pi/4$ at the core. At resonance it becomes $\pi/4$ and approaches its vacuum value after passing through the resonance.

The probability for an electron neutrino produced in the solar core to be detected as an electron neutrino on earth, averaged over the time of emission and the time of absorption, is given by

$$\langle P_{ee}\rangle = \cos^2\omega\cos^2\omega_m + \sin^2\omega\sin^2\omega_m - x_{12}\cos 2\omega\cos 2\omega_m, \tag{7}$$

where ω_m is to be evaluated at the point of production and x_{12} is the probability of a nonadiabatic jump between the matter-dependent mass eigenstates. If the variation of the solar density in the resonance region is slow enough, the adiabatic condition

$$\gamma \equiv \frac{\delta_{21}}{E|\frac{1}{A}\frac{dA}{dr}|_{\rm res}}\frac{\sin^2 2\omega}{\cos 2\omega} \gg 1 \tag{8}$$

is satisfied, the matter-dependent mass eignestates evolve adiabatically, and there are no transitions between them. If (8) is not satisfied, then there will be nonadiabatic transitions between the two matter-dependent mass eigenstates in the resonance region and the probability of this jump has the general form $\exp(-C/E)$. The term C has dimensions of energy and is some function of δ_{21}, ω, and the derivative of the solar density. The expressions for C for various density profiles are tabulated in Ref. [22]. For linear density variation in the resonance region, the jump probability is given by the Landau-Zener formula

$$x_{12} = \exp\left[-\frac{\pi}{2}\gamma\right]. \tag{9}$$

The predictions for the rates of various experiments are obtained by convoluting the SSM neutrino fluxes with the expression for survival probability in (7). A fit to the data from ^{71}Ga, ^{37}Cl, and Kamiokande experiments yields solutions in two regions in the δ_{21}-sin$^2 2\omega$ plane, one with small vacuum mixing and one with large vacuum mixing:

$$\delta_{21} \simeq 6.1\times 10^{-6}\,\text{eV}^2 \text{ and } \sin^2 2\omega \sim 0.0065,$$
$$\delta_{21} \simeq 9.4\times 10^{-6}\,\text{eV}^2 \text{ and } \sin^2 2\omega \sim 0.62. \tag{10}$$

In the case of the small mixing angle solution, the resonance occurs for neutrinos with energy greater than 0.6 MeV. Therefore, the p-p neutrinos (whose maximum energy is 0.42 MeV) are unaffected whereas the neutrinos with energy greater than 0.6 MeV are almost completely converted into ν_μ. But the measurement of Kamiokande shows that the neutrinos with energy greater than 7.5 MeV are suppressed by only a factor of 0.5. This can be accommodated through the nonadiabatic jump x_{12} in (7). If $C \simeq 10$ MeV, or equivalently $\delta_{21}\sin^2 2\omega \sim 4\times 10^{-8}$ eV^2, then x_{12} is negligible for energies less than 5 MeV, but becomes appreciable at higher energies, and $\langle P_{ee}\rangle$ satisfies Kamiokande constraint. The energy dependence of $\langle P_{ee}\rangle$ in this case is precisely of the form that is required to satisfy the data from the three solar neutrino experiments. In the case of the large angle solution, the nonadiabatic effects are totally negligible and the $\langle P_{ee}\rangle$ is about 0.55 below 0.5 MeV and slowly falls to about 0.35 around 5 MeV, after which it remains almost independent of the neutrino energy.

In the case of two flavor oscillations, the area of the parameter space which can satisfy all the three constraints at the 1σ level is very small. Especially in the case of the

small angle solution, the requirement that the resonance should occur around 0.6 MeV uniquely fixes the value of δ_{21}. The requirement that the ^{7}Be neutrinos should be completely suppressed and that the high energy ^{8}B neutrinos should have a suppression of about 0.5 determines the product $\delta_{21}\sin^2 2\omega$ almost exactly. Therefore there is very little leeway in the allowed values of δ_{21} and $\sin^2 2\omega$. An appreciable region of parameter space is allowed only at the 95% C.L. (or the 2.4 σ level). In addition, this simple picture is inadequate to simultaneously explain the solar and atmospheric neutrino deficits since the mass squared differences required are in vastly different regimes. To explain the atmospheric neutrino anomaly on the basis of two flavor vacuum oscillations, one requires a mass squared difference of the order of $10^{-1} - 10^{-3}$ eV^2, with a large mixing angle. This must be compared with the best fit to the data in the case of the solar neutrino problem given in Eq. (10). Therefore one has necessarily to consider the scenario in which all three neutrinos participate. This of course is also a more realistic situation since the experiments at the CERN e^+e^- collider LEP have already pinned down the number of light neutrino generations to be three.

Three flavor oscillations were considered previously [23–25]. However, the uncertainties in the gallium experiments have come down significantly in recent times and the parameter region allowed by the current data will be much smaller. Recently Joshipura and Krastev [26] have attempted a complete solution of the solar and atmospheric neutrino problems in the three generation framework. They present a combined analysis of these two problems in the framework of the MSW effect and indeed show that there exists a parameter space in which both sets of data can be reconciled. Giunti *et al.* [27] analyse these two problems and present a solution based on maximally mixed (in vacuum) three generations of neutrinos. This latter analysis is, however, a rather fine tuned solution since the parameter space allowed is rather tiny.

In this paper, we analyze the solar neutrino problem by considering the oscillations between the three neutrino flavors. The analysis is done with no particular model of neutrino masses and mixings assumed. The analysis is similar in spirit to that of Joshipura and Krastev [26]. We carry their analysis further and not only map out the full parameter space, but also discuss the average survival probability and recoil electron spectrum. In addition we also discuss a nonstandard solution where no resonance occurs but nevertheless there is a parameter space in which all the three experiments discussed earlier can be reconciled. We also do not make any assumption about the evolution being adiabatic and take into account nonadiabatic effects. These effects may be ignored, however, in parts of allowed parameter space. In the three generation case the neutrino oscillations are determined by two mass differences and three mixing angles neglecting the CP-violating phase. One of the mixing angles is irrelevant for the solar neutrino problem [23,24] while being relevant to the atmospheric neutrino problem and one of the mass differences is constrained by the atmospheric neutrino deficit. Therefore the solar neutrino oscillations in the three flavor case are dependent on three parameters. Because of the additional parameter, a larger region of the parameter space is allowed by the solar neutrino data compared to the two generation scenario. In Sec. II, we present the theoretical framework for our analysis of the solar neutrino problem and in Sec. III we present the numerical results for the solar neutrino problem in conjunction with the atmospheric neutrino problem. The last section consists of a brief summary and discussion.

II. THREE NEUTRINO OSCILLATIONS IN MATTER—A PERTURBATIVE ANALYSIS

In this section we discuss the mixing between three flavors of neutrinos and obtain the probability for a ν_e produced in the sun to be detected as a ν_e on earth. The three flavor eigenstates are related to the three mass eigenstates in vacuum through a unitary transformation:

$$\begin{bmatrix} \nu_e \\ \nu_\mu \\ \nu_\tau \end{bmatrix} = U^v \begin{bmatrix} \nu_1^v \\ \nu_2^v \\ \nu_3^v \end{bmatrix}, \tag{11}$$

where the superscript v on the right-hand side (RHS) stands for vacuum. The 3×3 unitary matrix U^v can be parametrized by three Euler angles (ω, ϕ, ψ) and a phase. The form of the unitary matrix can therefore be written in general as

$$U^v = U_{\text{phase}} U_{23}(\psi) U_{13}(\phi) U_{12}(\omega),$$

where $U_{ij}(\theta_{ij})$ is the mixing matrix between the ith and jth mass eigenstates with the mixing angle θ_{ij}. It has been shown that the expression for electron neutrino survival probability, integrated over the time of emission and of absorption, is independent of the phase and the third Euler angle ψ [23,24]. They can be set to zero without loss of generality and we have the following form for U^v:

$$U^v = \begin{pmatrix} c_\phi c_\omega & c_\phi s_\omega & s_\phi \\ -s_\omega & c_\omega & 0 \\ -s_\phi c_\omega & -s_\phi s_\omega & c_\phi \end{pmatrix}, \tag{12}$$

where $s_\phi = \sin\phi$ and $c_\phi = \cos\phi$, etc. The angles ω and ϕ can take values between 0 and $\pi/2$. Note that one of the flavors decouples if either ω or ϕ is zero and we have a two flavor scenario. As mentioned earlier the approach here is similar to that of Joshipura and Krastev [26] who, however, assume that the mixing angle between the second and third generations, ψ, is small and hence can be neglected. We wish to emphasize that this is not an assumption and in fact ψ can be arbitrary and the result for survival probability of the electron neutrino is independent of this [23,24]. In fact the solution of the atmospheric neutrino deficit requires ψ to be rather large. Together, solutions of the atmospheric neutrino deficit and the solar neutrino problem determine the mixing matrix U^v completely apart from the CP-violating phase.

The masses of the vacuum eigenstates are taken to be μ_1, μ_2, and μ_3. In the mass eigenbasis, the (mass)^2 matrix is diagonal:

$$M_0^2 = \begin{pmatrix} \mu_1^2 & 0 & 0 \\ 0 & \mu_2^2 & 0 \\ 0 & 0 & \mu_3^2 \end{pmatrix} = \mu_1^2 I + \begin{pmatrix} 0 & 0 & 0 \\ 0 & \delta_{21} & 0 \\ 0 & 0 & \delta_{31} \end{pmatrix}, \quad (13)$$

where $\delta_{21} = \mu_2^2 - \mu_1^2$ and $\delta_{31} = \mu_3^2 - \mu_1^2$. Without loss of generality, we can take δ_{21} and δ_{31} to be greater than zero. Neutrino oscillation amplitudes are independent of the first term so we drop it from further calculation. In the flavor basis the (mass)^2 matrix has the form

$$M_v^2 = U^v M_0^2 U^{v\dagger} = \delta_{31} M_{31} + \delta_{21} M_{21}, \quad (14)$$

where

$$M_{31} = \begin{pmatrix} s_\phi^2 & 0 & s_\phi c_\phi \\ 0 & 0 & 0 \\ s_\phi c_\phi & 0 & c_\phi^2 \end{pmatrix},$$

$$M_{21} = \begin{pmatrix} c_\phi^2 s_\omega^2 & c_\phi s_\omega c_\omega & -c_\phi s_\phi s_\omega^2 \\ c_\phi s_\omega c_\omega & c_\omega^2 & -s_\phi s_\omega c_\omega \\ -c_\phi s_\phi s_\omega^2 & -s_\phi s_\omega c_\omega & s_\phi^2 s_\omega^2 \end{pmatrix}. \quad (15)$$

As in the two flavor case, matter effects can be included by adding $A(r)$, defined in (4), to the e-e element of M_v^2. The matter corrected (mass)^2 matrix in the flavor basis is

$$M_m^2 = \delta_{31} M_{31} + \delta_{21} M_{21} + A M_A, \quad (16)$$

where

$$M_A = \begin{pmatrix} 1 & 0 & 0 \\ 0 & 0 & 0 \\ 0 & 0 & 0 \end{pmatrix}. \quad (17)$$

To calculate the evolution of a neutrino in matter we have to find the matter corrected eigenstates by diagonalizing M_m^2. For arbitrary values of δ_{31} and δ_{21}, it is cumbersome to find the eigenvalues and eigenvectors of M_m^2 algebraically. However, the eigenvalue problem can be solved using perturbation theory, if the mass differences have the hierarchy $\delta_{31} \gg \delta_{21}$. This assumption is plausible in light of the observed atmospheric muon neutrino deficit. Recently Kamiokande analyzed their atmospheric neutrino data, assuming that the deficit is caused by the oscillation of a ν_μ into another flavor. Their analysis assumes mixing between only two flavors ($\nu_\mu \leftrightarrow \nu_e$ or $\nu_\mu \leftrightarrow \nu_\tau$). For both cases their best fit yields a mass square difference of the order of 10^{-2} eV^2 [11]. In our analysis we take δ_{31} to be 10^{-2} eV^2. Thus we have δ_{31} much larger than $A_{\max}$ and hence the oscillations involving the third generation are not influenced very much by the matter effects. In order for the matter effects to be significant (as necessitated by the solar neutrino problem), the other mass difference in the problem, δ_{21}, should be such that the resonance condition is satisfied for some values of parameters. This means $\delta_{21} \sim A_{\max}$. Thus we work in an approximation where $\delta_{21}, A_{\max} \ll \delta_{31}$.

In this approximation, to the zeroth order, both the matter term and the term proportional to δ_{21} can be neglected in Eq. (16). Then $M_m^2 = \delta_{31} M_{31}$, whose eigenvalues and eigenvectors are

$$0; \begin{pmatrix} c_\phi \\ 0 \\ -s_\phi \end{pmatrix}, \quad 0; \begin{pmatrix} 0 \\ 1 \\ 0 \end{pmatrix}, \quad \delta_{31}; \begin{pmatrix} s_\phi \\ 0 \\ c_\phi \end{pmatrix}. \quad (18)$$

Treating $AM_A + \delta_{21} M_{21}$ as a perturbation to the dominant term in M_m^2 and carrying out degenerate perturbation theory, we get the matter-dependent eigenvalues and eigenvectors:

$$m_1^2; \begin{pmatrix} c_{\phi_m} c_{\omega_m} \\ -s_{\omega_m} \\ -s_{\phi_m} c_{\omega_m} \end{pmatrix}, \quad m_2^2; \begin{pmatrix} c_{\phi_m} s_{\omega_m} \\ c_{\omega_m} \\ -s_{\phi_m} s_{\omega_m} \end{pmatrix}, \quad m_3^2; \begin{pmatrix} s_{\phi_m} \\ 0 \\ c_{\phi_m} \end{pmatrix}. \quad (19)$$

The above eigenvectors are the columns of the unitary matrix U^m which relates the flavor eigenstates to matter-dependent mass eigenstates ν_i^m through the relation

$$\begin{bmatrix} \nu_e \\ \nu_\mu \\ \nu_\tau \end{bmatrix} = U^m \begin{bmatrix} \nu_1^m \\ \nu_2^m \\ \nu_3^m \end{bmatrix}. \quad (20)$$

The matter-dependent mixing angles can be expressed in terms of the vacuum parameters and A as

$$\tan 2\omega_m = \frac{\delta_{21} \sin 2\omega}{\delta_{21} \cos 2\omega - A \cos^2 \phi}, \quad (21)$$

$$\sin \phi_m = \sin \phi \left[1 + \frac{A}{\delta_{31}} \cos^2 \phi \right], \quad \cos \phi_m = \cos \phi \left[1 - \frac{A}{\delta_{31}} \sin^2 \phi \right]. \quad (22)$$

The matter-dependent eigenvalues m_i^2 are given by

$$m_1^2 = A \cos^2 \phi \cos^2 \omega_m + \delta_{21} \sin^2 (\omega - \omega_m),$$
$$m_2^2 = A \cos^2 \phi \sin^2 \omega_m + \delta_{21} \cos^2 (\omega - \omega_m),$$
$$m_3^2 = \delta_{31} + A \sin^2 \phi \simeq \delta_{31}. \quad (23)$$

ω_m can undergo a resonance if the values of δ_{21}, ϕ, and ω are such that the resonance condition

$$A(r) \cos^2 \phi = \delta_{21} \cos 2\omega \quad (24)$$

is satisfied for some r [22]. Note that this condition is very similar to the resonance condition in the two flavor case [Eq. (6)]. The new feature here, which occurs due to the mixing among the three neutrino flavors, is the presence of the second mixing angle ϕ in the resonance condition. This dependence on ϕ leads to a larger region of allowed parameter space in the three flavor oscillation scenario as will be shown in the next section. Since δ_{21}, $A(r)$, and $\cos^2\phi$ are all positive, a resonance can occur only if $\cos 2\omega$ is also positive, or if $\omega < \pi/4$.

In the three flavor case, the electron neutrino survival probability is given by

$$\langle P_{ee}\rangle = \sum_{i,j=1}^{3} |U_{ei}^{v}|^2 \, |U_{ej}^{m}|^2 \, |\langle \nu_i^v \mid \nu_j^m\rangle|^2. \tag{25}$$

$|\langle \nu_i^v \mid \nu_j^m\rangle|^2$ is the probability that the jth matter-dependent eigenstate evolves into the ith vacuum eigenstate. As in the two flavor case, if the adiabatic approximation holds, then

$$|\langle \nu_i^v \mid \nu_j^m\rangle|^2 = \delta_{ij}. \tag{26}$$

We introduce the jump probabilities

$$x_{ij} = |\langle \nu_i^v \mid \nu_j^m\rangle|^2 \quad \text{for } i \neq j \tag{27}$$

to take into account the nonadiabatic transitions, if the adiabatic condition does not hold.

Because $\delta_{31} \gg A_{\max}, \delta_{21}$, the third eigenvalue, both in vacuum and in matter, is much larger than the other two eigenvalues. Nonadiabatic effects are significant only if the eigenvalues of two states come close together [28]. Therefore the jump probabilities involving the third state, x_{13} and x_{23}, are expected to be negligibly small. Thus we have the expression for electron neutrino survival probability to be

$$\begin{aligned}\langle P_{ee}\rangle = {} & \cos^2\phi\cos^2\phi_m\left(\cos^2\omega\cos^2\omega_m + \sin^2\omega\sin^2\omega_m\right) \\ & + \sin^2\phi\sin^2\phi_m \\ & - x_{12}\cos^2\phi\cos^2\phi_m\cos 2\omega\cos 2\omega_m.\end{aligned} \tag{28}$$

For x_{12} we use the formula

$$x_{12} = \frac{\exp[-\frac{\pi\gamma F}{2}] - \exp[-\frac{\pi\gamma F}{2\sin^2\omega}]}{1 - \exp[-\frac{\pi\gamma F}{2\sin^2\omega}]}, \tag{29}$$

where γ is defined in Eq. (8) and

$$F = 1 - \tan^2\omega \tag{30}$$

for an exponentially varying solar density [22]. We use this form for the jump probability since it is valid for both large and small mixing angles. In the extreme nonadiabatic limit $x_{12} \to \cos^2\omega$ and when $\gamma F >> 1$ we have the usual Landau-Zener jump probability given by $x_{12} \to \exp[-\frac{\pi\gamma F}{2}]$ as expected. In fact, for much of the allowed parameter space, this form can be used without any appreciable change in the results obtained.

III. RESULTS

In this section we discuss the results of the numerical analysis first for the solar neutrino problem and using that we map out the region in the parameter space which contains the solution to the atmospheric neutrino problem.

A. Solar neutrinos

We analyze the expression for $\langle P_{ee}\rangle$ in (28) and find the ranges of δ_{21}, ω, and ϕ allowed by the three solar neutrino experiments. Since $\delta_{31} \gg A_{\max}$, we see from the expression for ϕ_m in (22) that the angle ϕ is almost unaffected by the matter effects. However, ω_m can be significantly different from ω and can undergo resonance if the resonance condition in (24) is satisfied. Since this resonance condition depends on ϕ, in addition to δ_{21} and ω, a larger region of parameter space satisfies the three constraints from the experiments.

To search for the regions allowed in the three parameter space δ_{21}, ω, and ϕ, we define the suppression factors observed by the three types of experiments,

$$\begin{aligned} y_{\mathrm{Ga}} &= \frac{R_{\mathrm{Ga\,avg}}}{\mathrm{R}_{\mathrm{Ga\,SSM}}} = 0.563 \pm 0.067, \\ y_{\mathrm{Cl}} &= \frac{R_{\mathrm{Cl}}}{R_{\mathrm{Cl\,SSM}}} = 0.318 \pm 0.051, \\ y_{\mathrm{Kam}} &= \frac{R_{\mathrm{Kam}}}{R_{\mathrm{Kam\,SSM}}} = 0.51 \pm 0.07, \end{aligned} \tag{31}$$

where the first number refers to the average of the data given by two experiments—namely, GALLEX and SAGE. The predicted SSM rates for various experiments were taken from Bahcall-Pinsonneault SSM calculations [3]. The uncertainties in y_i are the sum of the experimental uncertainty in the numerator and the theoretical uncertainty in the denominator, added in quadrature.

The predictions for y_i for the three flavor oscillation scenario are obtained by convoluting the SSM fluxes and the detector cross sections with $\langle P_{ee}\rangle$ from (28). The expression we use is

$$y = \frac{\sum_K \int_{E_{\min}}^{E_{\max}} dE\Phi_K(E)\sigma(E)\langle P_{ee}\rangle(E)}{\sum_K \int_{E_{\min}}^{E_{\max}} dE\Phi_K(E)\sigma(E)}, \tag{32}$$

where the sum over K refers to the neutrino fluxes from various sources contributing to the process. We also include the contributions from the CNO cycle apart from the dominant contributions from the p-p cycle. In the case of Kamioka, only the ^{8}B flux contributes and one must also take into account the neutral current contribution arising from the muon neutrinos interacting with the detector material. The parameter ranges are then calculated by putting vetos on y at 1σ and 1.6σ levels. The energy-dependent fluxes were taken from Ref. [3] and the

cross sections were taken from Ref. [29].

Figure 1 shows the allowed values of ω and ϕ with δ_{21} varying between 10^{-6} eV^2 and 10^{-4} eV^2. Note that the allowed values of δ_{21} are also determined by the same veto conditions. In the two generation case it is a standard practice to plot δ_{21} against $\sin^2(2\omega)$ since that is the combination that enters the survival probability. In the three generation case all possible circular functions of the mixing angles are possible. Hence we depart from the standard practice in this paper and plot the angles themselves. The points refer to the allowed values after the vetos corresponding to all three experiments are imposed. The dark squares show the values allowed by 1σ uncertainties given in (31) whereas the hollow squares show the values allowed when the uncertainty is increased to 1.6σ. Figure 2 shows the allowed regions in the ϕ-δ_{21} plane, with ω varying between 0 and $\pi/2$ but obeying the same set of vetos. In Figs. 1 and 2 if we restrict ourselves to the $\phi = 0$ lines (the y axes) we get the known [2] two flavor solutions for ω and δ_{21}. The large extended regions of the parameter space brought in through the additional degree of freedom ϕ in the three flavor scenario are shown clearly in Figs. 1 and 2. For completeness we also plot in Fig. 3 the allowed range in the ω-δ_{21} plane. Here again the three flavor scenario provides an enlargement of the allowed parameter space over that of the two flavor solution (small regions around the isolated dark patch in the left and around the end of the dark arm on the right).

The various regions of the allowed parameter space may be classified as follows: (1) small δ_{21}, small ω, small ϕ, (2) large δ_{21}, large ω, small ϕ, (3) small δ_{21}, small ω, large ϕ, (4) large δ_{21}, small ω, large ϕ, (5) large δ_{21}, large ω, large ϕ, where the small or large δ_{21} means either $\delta_{21} < 10^{-5}$ eV^2 or $\delta_{21} > 10^{-5}$ eV^2. The first two regions corresponding to small ϕ in the above classification belong to an approximate two generation situation since the angle ϕ is small. The one corresponding to small ω is the usual nonadiabatic solution, whereas the one corresponding to large ω is the usual adiabatic solution. The rest invoke the genuine three generation oscillation mechanism. In the two flavor scenario, the small angle solution (corresponding to ω small as in case 1 above) gives the best fit [2]. There the parameter space allowed at 1σ level is very small because the resonance condition

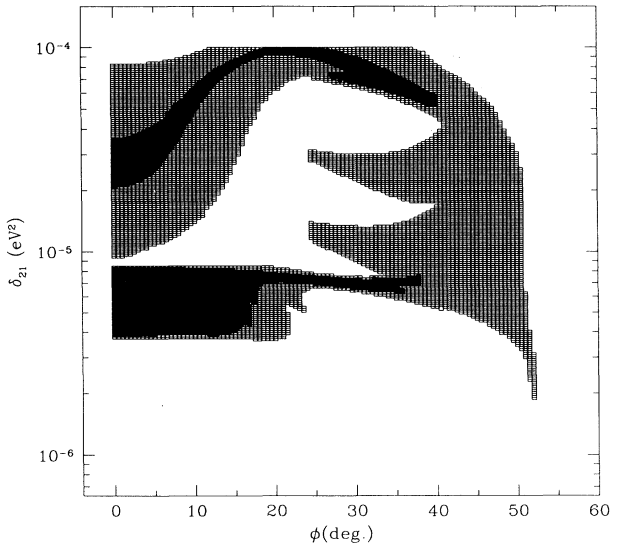

FIG. 2. Allowed regions in ϕ-δ_{21} plane (with $0 \leq \omega \leq \pi/2$) at 1σ (dark squares) and at 1.6σ (hollow squares).

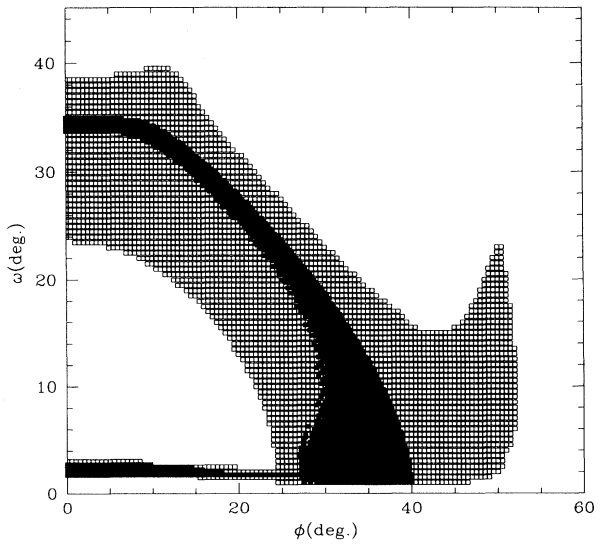

FIG. 1. Allowed regions in ϕ - ω plane (with 10^{-6} eV^2 $\leq \delta_{21} \leq 10^{-4}$ eV^2) at 1σ (dark squares) and at 1.6σ (hollow squares).

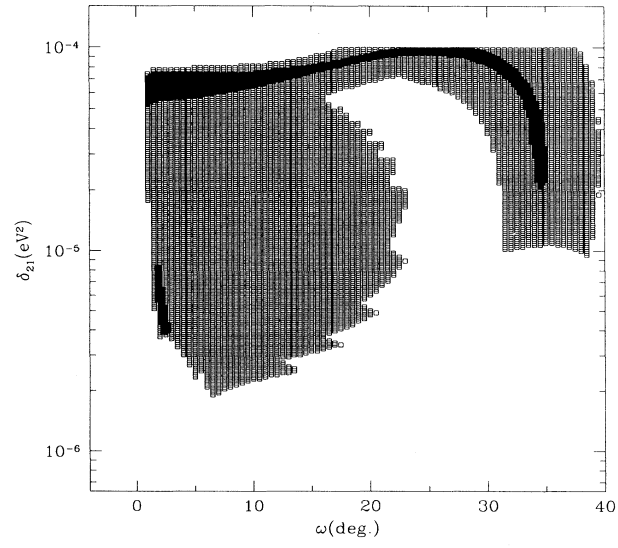

FIG. 3. Allowed regions in ω-δ_{21} plane ($0 \leq \phi \leq \pi/2$) at 1σ (dark squares) and at 1.6σ (hollow squares).

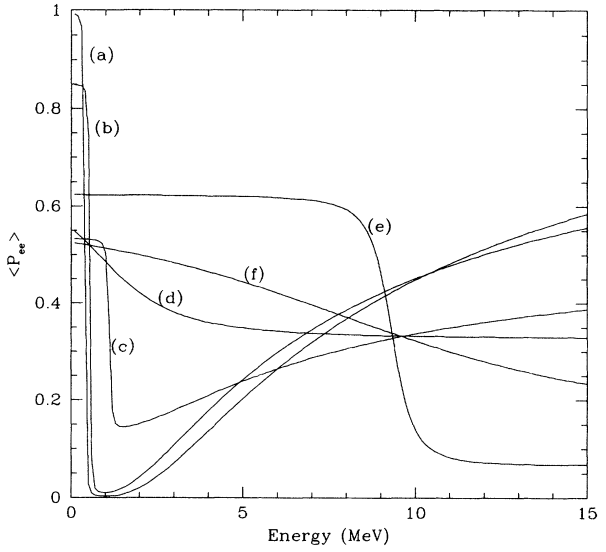

FIG. 4. Survival probability $\langle P_{ee} \rangle$ vs E_ν for typical values of ϕ, ω, and δ_{21} in the allowed region. The parameters chosen are (a) $\delta_{21} = 4.0 \times 10^{-6}$, $\omega = 2.5°$, $\phi = 2.0°$; (b) $\delta_{21} = 5.0 \times 10^{-6}$, $\omega = 2.0°$, $\phi = 16.5°$; (c) $\delta_{21} = 7.0 \times 10^{-6}$, $\omega = 1.75°$, $\phi = 37.5°$; (d) $\delta_{21} = 2.5 \times 10^{-5}$, $\omega = 35.0°, \phi = 3.0°$; (e) $\delta_{21} = 7.0 \times 10^{-5}$, $\omega = 2.0°, \phi = 30.0°$; (f) $\delta_{21} = 1.0 \times 10^{-4}$, $\omega = 24.5°$, $\phi = 24.0°$; δ_{21} is given in terms of eV^2.

and the nonadiabatic jump factor fix δ_{21} and ω almost uniquely. These values of parameters indicate that the neutrinos from the *p-p* cycle suffer very little suppression and those from ^{7}Be suffer almost complete suppression as will be illustrated soon in the analysis of the survival probability.

In the three flavor scenario, the resonance condition [Eq. (24)] and the survival probability [Eq. (28)] are dependent on the second angle ϕ also. The suppression of the *p-p* neutrinos depends on the value of ϕ and if this suppression is significant then the complete suppression for ^{7}Be neutrinos can be relaxed. This is one of the important differences between the three flavor and the two flavor oscillations.

Figure 4 shows the energy dependence of $\langle P_{ee} \rangle$ for some representative values of ω, ϕ , and δ_{21}. The curve labeled (a) corresponds to $\phi = 2°$. As there is very little mixing between the first and the third generations of neutrinos, this is in fact an almost two generation case. In agreement with the two generation analysis, there is almost no suppression of the *p-p* neutrinos and the ^{7}Be neutrinos are almost completely suppressed. The survival probability at the high energies relevant to Kamioka is almost a linear function with an average around 0.5 as one would expect. Also here the values of ω and δ_{21} are small (they are almost equal to the values obtained in the two flavor case) and the nonadiabatic effects become important beyond 2 MeV. Keeping ω small, if we increase ϕ in the allowed region there is a perceptible reduction in the probability in the *p-p* energy range and an increase in the survival probability of the ^{7}Be neutrinos [curves (b) and (c)]. When δ_{21} is increased, however, there is a qualitative change in the survival probability profile. In this range both ω and ϕ are allowed to be large. Here also there is a qualitative change when ω is small or large. For large ω the survival probability is a smooth function resembling the adiabatic case of the two generation analysis [curves (d) and (f)] whereas for small ω it is almost a step function [curve (e)] which is like the classic adiabatic case discussed by Bethe in the two generation case [19]. One common feature of the large δ_{21} case is that the *p-p* neutrinos undergo substantial suppression varying between 0.6 and 0.5. The resonance also occurs at a much higher energy than in the small δ_{21} case. Curve (f) has ω, ϕ, and δ_{21} all large and in some sense it can be called "most representative" of the three flavor oscillation scenario because both the mixing angles in this case are large. In all the above cases, except (e), the average survival probability above 7 MeV is in the neighborhood of 0.4 which is what is required by the Kamioka data and there is no dramatic change from one to the other. This is not so at low energies where the curves differ dramatically. In this sense the Kamioka experiment cannot distinguish between different theoretical scenarios of masses and mixings.

One way of experimentally measuring the energy dependence of $\langle P_{ee} \rangle$ is to look at the recoil electron spectrum in those detectors that use ν_e-e scattering. In Fig. 5 we have shown the recoil electron spectrum for the six cases plotted in Fig. 4. Except case (f), they cannot be distinguished beyond 10 MeV, whereas there are substantial differences at low energies. While this energy range is not completely accessible in Kamioka, it is interest-

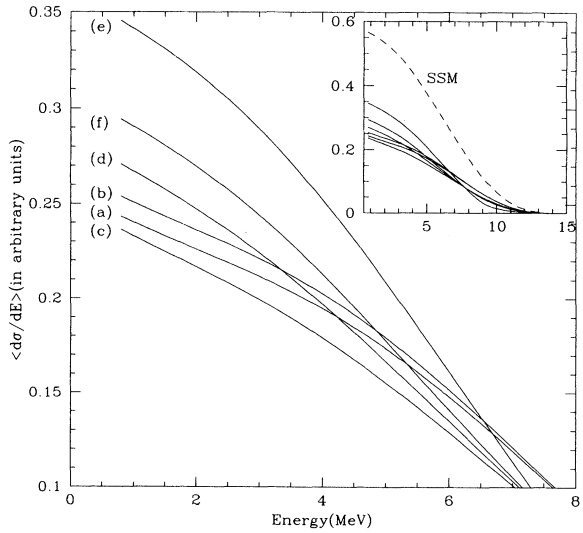

FIG. 5. Recoil electron spectrum for different representative points of the allowed parameter region. The parameters for the different curves labeled (a)–(f) are the same as in Fig. 4. The inset shows a comparison of all six cases with the SSM spectrum (dashed line).

ing to note that it may be possible to see this difference in the experimental recoil electron spectrum in the SNO [30] and Borexino [31] detectors. Note that in computing the recoil electron spectrum we have used the spectrum of ^{8}B neutrinos as input. This is because the threshold in experiments which can measure the recoil electron spectrum (such as SNO and Kamioka) is more than a few MeV's where only this flux matters. The only exception is Borexino where the threshold is much lower and there are other contributions below 1.5 MeV. In particular, the ^{7}Be neutrino source, which is a line spectrum at 0.862 MeV, will show up as a sharp bump in the recoil spectrum where the height of the bump depends on the survival probability. A complete absence of the bump would point to the set parameters as in case (a) of Fig. 4.

Finally we consider a nonstandard mixing which leads to a substantial region in the parameter space. We consider a situation where the electron neutrino is coupled more strongly to the heavier mass eigenstate ν_2. Obviously this implies that the mixing angle between the first two mass eigenstates, ω, is greater than $\pi/4$. In the standard analysis the mixing has to be less than $\pi/4$ so that the resonance condition is satisfied as can be seen from Eq. (24). This is true in the two as well as in the three generation case since the LHS of the resonance condition is positive for arbitrary ϕ whereas the sign in the RHS depends on the magnitude of ω. There are no strong theoretical reasons not to consider this situation. Because ω_m at core is very close to $\pi/2$, ω_m is then constrained to be $\omega \leq \omega_m < \pi/2$. In fact, for $\delta_{21} \leq 10^{-7}$ eV^2, ω_m is approximately $\pi/2$. Since ϕ hardly varies with density the effective survival probability may be approximately written as

$$\langle P_{ee} \rangle = \cos^4\phi \sin^2\omega + \sin^4\phi - x_{12}\cos^4\phi|\cos 2\omega|, \quad (33)$$

where we have retained the jump probability x_{12}. While it may appear somewhat unusual to keep the jump probability when there is no resonance, a plot of the eigenvalues clearly shows that the difference between the first two eigenvalues is not very different from that of the standard case close to vacuum and one cannot completely discard the existence of nonadiabatic jumps between mass eigenstates. However, most of the derivations of the jump probability assume the existence of resonance and the profile of the density variation close to resonance. Since we do not have a handle on this, we assume that the jump probability is simply given by $x_{12} = \exp(-C/E)$ and treat C as a free parameter of the theory. The survival probability is then energy dependent as would be required by the solution to the solar neutrino puzzle. The resulting parameter space is shown in Fig. 6 for ω, ϕ. The parameter C varies from 0.4 to 6.3 in the allowed region. If we assume any one of the expressions for the jump probability discussed earlier, then we will have to discard small values of C ($C < 4$) since then the jump probability becomes very large and unacceptable. However, in the allowed region, the points corresponding to small C are very few and there is no substantial change from the plot shown in Fig. 6. We also show some typical variation of the survival probability $\langle P_{ee} \rangle$ for some typical values of ω, ϕ, and C in Fig. 7. The curve (a) corresponds to small C where nonadiabatic effects are important while the curve (b) corresponds to large C which is an almost adiabatic case. We wish to stress that this is an *ad hoc* solution but we have analyzed this situation because there are no strong theoretical reasons to ignore

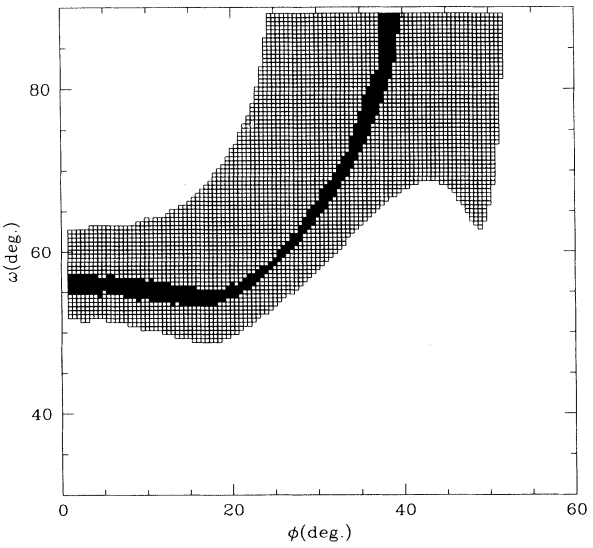

FIG. 6. Allowed regions in ϕ-ω plane (with $0.4 \leq C \leq 6.4$) (dark squares) and at 1.6σ (hollow squares) for the nonstandard solutions.

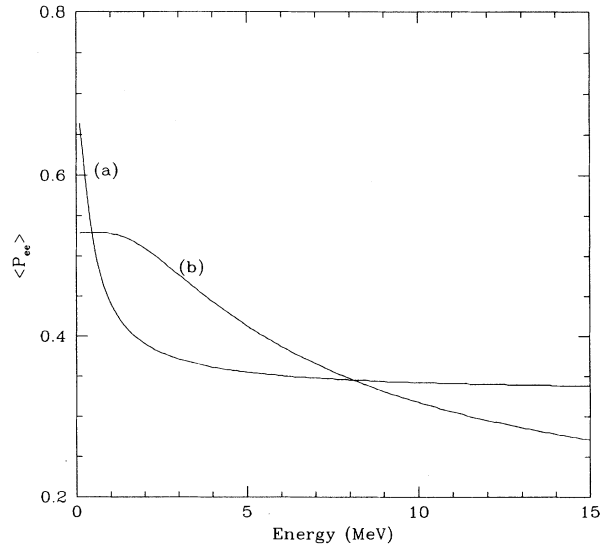

FIG. 7. Typical survival probability profile in the nonstandard case. The curve labeled (a) corresponds to $C = 0.4$, $\omega = 55°, \phi = 2°$ and the curve labeled (b) corresponds to $C = 6$, $\omega = 89°$, $\phi = 38°$.

this possibility.

To conclude this section, we note that the solution to the solar neutrino puzzle fixes the parameter space defined by ω, ϕ, and δ_{21}. While we have actually chosen the fourth parameter δ_{31} to be 10^{-2} eV^2 we might as well have set the limit $\delta_{31} > 10^{-3}$ eV^2 without affecting our results. One therefore requires more inputs to fix the range of δ_{31} and the angle ψ (mixing angle between the second and third generation neutrinos) which is arbitrary as far as the solar neutrino puzzle is concerned. The new input is provided by the analysis of the atmospheric neutrino problem which we consider next.

B. Atmospheric neutrinos

In order to fix the mixing matrix completely we still need to fix the range of ψ, which is the mixing angle between the second and third generation neutrinos, as this is arbitrary in the solar neutrino analysis. To have a consistent solution for both the solar neutrino and the atmospheric neutrino problems, we need to show that there exists a range of ψ in the allowed range of parameters occurring in the solar neutrino problem. The Kamiokande Collaboration presents its results in the form of the double ratio [11]

$$R = \frac{\left(\frac{N_{\nu_\mu}}{N_{\nu_e}}\right)_{\rm obs}}{\left(\frac{N_{\nu_\mu}}{N_{\nu_e}}\right)_{\rm MC}}. \tag{34}$$

The numerator of R is the observed ratio of muon type events to the electron type events and the denominator of R the Monte Carlo expectation of the same ratio in the absence of neutrino oscillations. For sub-GeV data ($E < 1.33$ GeV) $R = 0.60^{+0.07}_{-0.06} \pm 0.05$ and for multi-GeV data ($E > 1.33$ GeV) $R = 0.57^{+0.08}_{-0.07} \pm 0.07$. These two numbers are consistent with each other and seem to indicate that the suppression of atmospheric muon neutrinos is independent of energy. For sub-GeV data there is no zenith angle dependence whereas the multi-GeV data show some evidence that R depends on the zenith angle.

In the presence of oscillations, the number of muon type and electron type events can be written as

$$N_\mu = \int \phi_{\nu_\mu} P_{\mu\mu} \sigma_\mu dE + \int \phi_{\bar\nu_\mu} P_{\bar\mu\bar\mu} \sigma_{\bar\mu} dE + \int \phi_{\nu_e} P_{e\mu} \sigma_\mu dE + \int \phi_{\bar\nu_e} P_{\bar e\bar\mu} \sigma_{\bar\mu} dE, \tag{35}$$

$$N_e = \int \phi_{\nu_e} P_{ee} \sigma_e dE + \int \phi_{\bar\nu_e} P_{\bar e\bar e} \sigma_{\bar e} dE + \int \phi_{\nu_\mu} P_{\mu e} \sigma_e dE + \int \phi_{\bar\nu_\mu} P_{\bar\mu\bar e} \sigma_{\bar e} dE, \tag{36}$$

where ϕ's are the atmospheric neutrino fluxes, P_{ij}'s are the probabilities for neutrino of flavor i to oscillate into flavor j, and σ_i's are the charged current cross sections for the neutrinos of flavor i to interact with the material of the detector.

The energy dependence of the fluxes and the reaction cross sections are well known. The energy dependence of the P_{ij}'s is very complicated if the matter effects, including those arising from the density profile of earth, are taken into account. The matter effects are very important for the analysis of multi-GeV data which show a zenith angle dependence. This analysis is in progress. Here we consider only the sub-GeV data to keep the analysis simple. For sub-GeV energies, the matter effects are negligible. Hence we can use vacuum oscillation probabilities for P_{ij}'s:

$$\begin{aligned} P_{ij} = {} & U_{i1}^2 U_{j1}^2 + U_{i2}^2 U_{j2}^2 + U_{i3}^2 U_{j3}^2 \\ & + 2U_{i1}U_{i2}U_{j1}U_{j2} \cos\left(2.53 \frac{d\delta_{21}}{E}\right) \\ & + 2U_{i1}U_{i3}U_{j1}U_{j3} \cos\left(2.53 \frac{d\delta_{31}}{E}\right) \\ & + 2U_{i3}U_{i2}U_{j3}U_{j2} \cos\left(2.53 \frac{d\delta_{32}}{E}\right), \end{aligned} \tag{37}$$

where E is the energy given in units of MeV, δ_{ij} are the mass differences in eV^2, d is the distance of traversal in m, and the U's are the elements of the vacuum mixing matrix given in Eq. (12). In vacuum the oscillation probability for antineutrinos is the same as that for the neutrinos; i.e., $P_{\mu\mu} = P_{\bar\mu\bar\mu}$, $P_{ee} = P_{\bar e\bar e}$, etc. In Eq. (37) the cosine term containing δ_{21} can be set to unity because the maximum distance traveled by neutrinos ($\sim$ 13 000 km) is much smaller than the corresponding oscillation length. Since the sub-GeV data do not have zenith angle dependence, the cosine terms involving δ_{31} and δ_{32} can be replaced by the corresponding averages over d. This is possible only if many oscillation lengths are contained in the distance traveled by the neutrinos. This sets a lower limit on the mass difference $\delta_{31} > 10^{-3}$ eV^2. It is interesting to note that the same lower limit is needed on δ_{31} to satisfy the approximation we made in the solar neutrino analysis. Since the cosine terms in Eq. (37) are replaced by their average values, the exact value of δ_{31} is immaterial as long as it satisfies the above constraint.

We make one further approximation which simplifies the analysis considerably. The charged current cross sections σ_μ and σ_e, in general, have different energy dependence. However, it was shown [32] that $\sigma_\mu \simeq \sigma_e$ and $\sigma_{\bar\mu} \simeq \sigma_{\bar e}$ for $E_\nu > 200$ MeV. Using all these above approximations, the expression for R can simply be written as

$$R = \frac{P_{\mu\mu} + rP_{e\mu}}{P_{ee} + \frac{1}{r}P_{\mu e}}, \tag{38}$$

where

$$r = \frac{\int \left[\phi_{\nu_e}\sigma_e + \phi_{\bar\nu_e}\sigma_{\bar e}\right] dE}{\int \left[\phi_{\nu_\mu}\sigma_\mu + \phi_{\bar\nu_\mu}\sigma_{\bar\mu}\right] dE}. \tag{39}$$

r is simply the ratio of the number of electron type of events to the muon type events if there were no oscillations. Therefore we restrict our attention to the part of the data satisfying the constraint $E > 200$ MeV. The Kamiokande Collaboration [11] has given the values for r

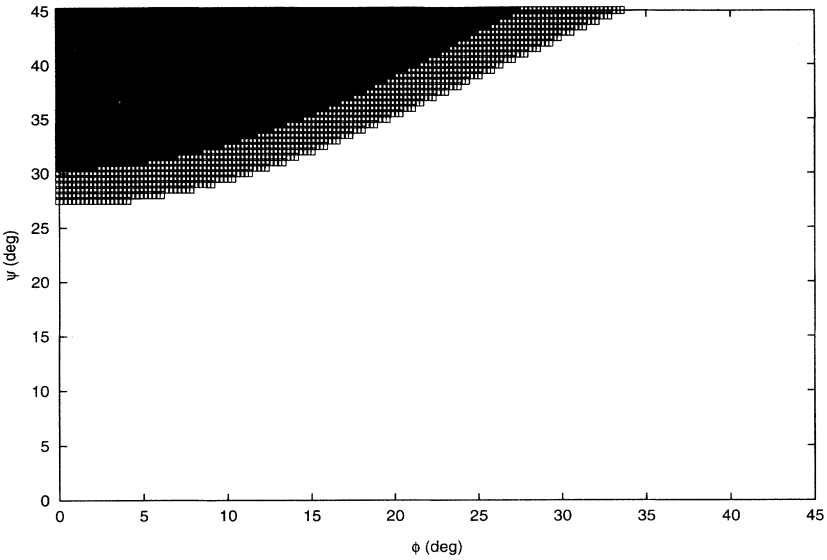

FIG. 8. The allowed range of values for the mixing angle ψ in the ψ-ϕ plane when ϕ and ω are restricted to the range allowed by the solar neutrino problem (see Fig. 1).

and R for different energy bins. By taking the weighted average of the results for bins with $E > 200$ MeV, we get

$$r = 0.523 \quad \text{and} \quad R = 0.533^{+0.07}_{-0.06} \pm 0.05. \tag{40}$$

We fix the range of ψ by requiring the theoretical value of R calculated from Eq. (38) to be within 1σ and 1.6σ of the experimental value. The resulting range for ψ is shown in Fig. 8, where as usual the full squares show the 1σ veto and the open squares show the 1.6σ veto.

A few comments are in order here. As in the two generation analysis of the atmospheric neutrino problem, we find that the preferred value of ψ is large and around $\pi/4$. This can be checked easily by looking at the conversion probability $P_{\mu e}$ in the allowed range of parameters for the atmospheric neutrino problem. It turns out that this conversion probability is always less than 20%. Thus the solution to the atmospheric neutrino problem is mainly driven by the ν_μ-ν_τ oscillations whereas the solution to the solar neutrino problem is mainly driven by ν_e-ν_μ oscillations at least for small values of ϕ. However there are large domains of the parameter space where one requires the full three generation analysis presented here to have a consistent solution to both the problems.

IV. SUMMARY AND DISCUSSION

We have examined in detail the possible solutions to the solar neutrino and atmospheric neutrino puzzles in the realistic three generation framework. There are in general three mixing angles, one phase from the mixing matrix, and two mass squared differences which define the full parameter space. In the case of solar neutrinos the survival probability for the electron neutrino, even after taking into account the matter effects, is independent of the phase and one of the mixing angles. We also fix one of the mass squared differences by appealing to the atmospheric neutrino problem. Thus our parameter space in the solar neutrino analysis consists of two angles and one mass squared difference. In our case these are chosen to be ω, which gives the mixing between first and second generations, ϕ, which is the mixing between first and third generations, and δ_{21}, which is the mass squared difference between the first two generations. The mass difference δ_{31} is fixed to be around 10^{-2} eV^2 to explain the atmospheric neutrino problem. We have mapped out the parameter space $(\phi, \omega, \delta_{21})$ by invoking the vetos arising from the data given by the three solar neutrino experiments. Next we have used these allowed ranges of parameters from the solar neutrino analysis as input in the atmospheric neutrino analysis to fix the angle ψ and find that there exists a substantial range in this parameter which allows a solution to the atmospheric neutrino puzzle. The numerical calculations necessarily depend on the bin size for the parameters. We have ensured that the bin size we have chosen is such that a further reduction will not change the overall profile of the allowed region. However, it is conceivable that the rough edges that one still sees in parts of the allowed region will be smoothed out by a further reduction of the bin size.

In conclusion, we have shown that there exists a consistent solution to the solar and atmospheric neutrino deficit puzzles within the framework of the standard MSW mechanism based on the set of all available measurements of the solar neutrino fluxes. The full analysis involves five parameters which we have mapped out by accommodating the solar and atmospheric neutrino fluxes seen by the present set of experiments. While the allowed region in the parameter space is still large, these can be constrained further by measuring the distributions of recoil electron energies in solar neutrino detectors that use ν-e scattering. Although the threshold energy at the Kamioka detector is rather too high for this purpose, the SNO and Borexino detectors may be effective in narrowing the parameter space. Finally we would like to remark that the analysis of solar and atmospheric neutrino problems presented here is exploratory in nature. This is so

since with time the errors are bound to change, which in turn will affect the vetos imposed by us at 1σ and 1.6σ levels. Nevertheless we believe there is already sufficient indication that a robust solution of both problems is possible within the framework provided by the mechanism of neutrino oscillations with three generations.

After finishing this work we learned that a similar analysis was carried out by Fogli, Lisi, and Montanino [33]. Their results agree with ours.

ACKNOWLEDGMENTS

This work was started during the Third Workshop on High Energy Particle Physics (WHEPP 3) in Madras. We gratefully acknowledge the collaboration in the initial stages with Professor A. S. Joshipura. We also thank Professor K. V. L. Sarma for keeping us informed of the recent developments in neutrino oscillations.

[1] K. V. L. Sarma, Int. J. Mod. Phys. A **10**, 767 (1995).
[2] P. Langacker, Invited talk presented at 32nd International School of Subnuclear Physics, Erice, 1994, Report No. UPR-0640T, 1994, hep-ph/9411339 (unpublished).
[3] J. N. Bahcall and M. H. Pinsonneault, Rev. Mod. Phys. **64**, 885 (1992).
[4] K. Lande, in *Neutrino 94*, Proceedings of the 16th International Conference on Neutrino Physics and Astrophysics, Eilat, Israel, edited by A. Dar, G. Eilam, and M. Gronau [Nucl. Phys. B (Proc. Suppl.) **38** (1995)].
[5] M. Nakahata, in *Proceedings of the 27th International Conference on High Energy Physics*, Glasgow, Scotland, 1994, edited by P. J. Bussey and I. G. Knowles (IOP, London, 1995).
[6] P. Anselman *et al.*, Phys. Lett. B **327**, 377 (1994).
[7] J. S. Nico, in *Proceedings of the 27th International Conference on High Energy Physics* [5].
[8] N. Hata and P. Langacker, Phys. Rev. D **52**, 420 (1995).
[9] W. Kwong and S. P. Rosen, Phys. Rev. Lett. **73**, 369 (1994).
[10] Stephen Parke, Phys. Rev. Lett. **74**, 839 (1995).
[11] Kamiokande Collaboration, K. S. Hirata *et al.*, Phys. Lett. B **280**, 146 (1992); Kamiokande Collaboration, Y. Fukuda *et al.*, *ibid.* **335**, 237 (1994).
[12] D. Casper *et al.*, Phys. Rev. Lett. **66**, 2561 (1991); R. Becker-Szendy *et al.*, Phys. Rev. D **46**, 3720 (1992).
[13] M. Aglietta *et al.*, Europhys. **8**, 611 (1989).
[14] Ch. Berger *et al.*, Phys. Lett. B **245**, 305 (1990).
[15] M. Goodman, Talk at the atmospheric neutrino workshop, Louisiana, 1993 (unpublished).
[16] A. Acker, J. G. Learned, S. Pakvasa, and T. J. Weiler, Phys. Lett. B **298**, 149 (1993).
[17] S. M. Bilenky and B. Pontecorvo, Phys. Rep. **41**, 225 (1978).
[18] L. Wolfenstein, Phys. Rev. D **17**, 2369 (1978); **20**, 2634 (1979); S. P. Mikheyev and A. Yu. Smirnov, Yad. Fiz. **42**, 1441 (1985) [Sov. J. Nucl. Phys. **42**, 913 (1985)]; Nuovo Cimento C **9**, 17 (1986).
[19] H. A. Bethe, Phys. Rev. Lett. **56**, 1305 (1986).
[20] J. N. Bahcall and H. A. Bethe, Phys. Rev. Lett. **65**, 2233 (1990).
[21] N. Hata and P. Langacker, Phys. Rev. D **50**, 632 (1994).
[22] T. K. Kuo and J. Pantaleone, Rev. Mod. Phys. **61**, 937 (1989).
[23] T. K. Kuo and J. Pantaleone, Phys. Rev. D **35**, 3432 (1987).
[24] A. S. Joshipura and M. V. N. Murthy, Phys. Rev. D **37**, 1374 (1988).
[25] D. Harley, T. K. Kuo, and J. Pantaleone, Phys. Rev. D **47**, 4059 (1993).
[26] A. S. Joshipura and P. I. Krastev, Phys. Rev. D **50**, 3484 (1994).
[27] C. Giunti, C. W. Kim, and J. D. Kim, Phys. Lett B **352**, 357 (1995).
[28] L. D. Landau and E. M. Lifshitz, *Non-relativistic Quantum Mechanics*, 3rd ed.(Pergamon Press, Oxford, 1977).
[29] J. Bahcall, *Neutrino Astrophysics* (Cambridge University Press, Cambridge, England, 1989).
[30] G. T. Ewan *et al.*, Sudbury Neutrino Observatory Proposal, Report No. SNO-87-12, 1987 (unpublished).
[31] "Borexino at Gran Sasso," Proposal for a real time detector for low energy solar neutrinos, edited by G. Bellini, M. Campanella, D. Guigni, and R. S. Raghavan, 1991 (unpublished).
[32] A. K. Mann, Phys. Rev. D **48**, 422 (1993).
[33] G. L. Fogli, E. Lisi, and D. Montanino, Phys. Rev. D **49**, 3626 (1994); CERN Report No. CERN-TH-7491/94 (unpublished).